Energy Efficiency Maximization for Multi-Node IoT Networks Operating with Finite Blocklength Codes

(Invited Paper)

Yizhen Zhao[†,‡], Wei Gao[†,‡], Yao Zhu[†,‡], Yulin Hu[†,‡] and James Gross[¶]
[†]School of Electronic Information, Wuhan University, China, Email: $yizhen.zhao|wei.gao|yulin.hu$@whu.edu.cn
[‡]INDA Institute, RWTH Aachen University, Germany, Email: zhu@inda.rwth-aachen.de
¶KTH Royal Institute of Technology, Stockholm, Sweden, Email: $jamesgr$@kth.se

***Abstract*—In this paper, we consider an Internet of Things (IoT) network supporting latency-critical transmissions to multiple nodes in the finite blocklength regime. An energy efficiency maximizing design is provided via efficiently jointly allocating the power and blocklength among the transmissions to different nodes, while guaranteeing per-node constraint of reliability. To address the formulated non-convex problem, we propose a Majorization-Minimization-based approach. Specifically, we tightly approximate the problem at each local point by introducing an auxiliary constant. Then, we rigorously prove the convexity of the conducted local problem. By successively optimally solving each convex local problem, a near-optimal solution is finally achieved. Via simulations, we demonstrate the performance advantages of the proposed joint design.**

***Index Terms*—energy efficiency, finite blocklength, resource allocation, multi-node, 6G**

I. Introduction

Future industrial Internet of Things (IoT) networks are expected to support latency-critical connections to IoT devices while guaranteeing high reliability of transmissions [1], [2]. In addition, the deployments of IoT devices are exponentially increasing, which provides significant difficulties for IoT system designs [3], [4]. On the one hand, with limited radio frequency resources, it becomes more challenging to guarantee latency and reliability-critical communications to more IoT nodes. On the other hand, the sharply increased energy consumption of the network raises the issue that a smart tradeoff between energy consumption and transmission performance (reliability, latency, and so on) should be achieved and that the energy efficiency (EE) of the Industrial IoT network should be enhanced.

Several studies provide EE improvements for IoT networks from different perspectives. A max-energy-efficiency approach under narrowband IoT link adaptation is investigated in [5]. To solve the EE maximization problem in the IoT region, the alternating direction method of multipliers (ADMM) is adopted in [6]. The authors in [7] provide an EE enhancement method by introducing an efficient power control algorithm. In [8], an energy-efficient scheduling design is presented to improve the transmission efficiency and working time for IoT nodes. In addition, the work in [9] proposes a dynamic resources allocation scheme by instantaneously determining time and power among IoT nodes to reduce the total energy consumption.

All of the above research is conducted with the assumption that transmission is arbitrarily reliable under Shannon's capacity, which is true only when the blocklength of the transmission is infinite. Unfortunately, industrial IoT devices usually transmit short data packets, and the transmission is usually carried by short blocklength codes due to the latency-critical requirements [10], [11]. In other words, such transmissions are operated in the so-called finite blocklength (FBL) regime. To characterize the relation of coding rate, error probability, as well as blocklength, Polyanskiy in [12] proposed an accurate approximation of FBL communications. According to Polyanskiy's model [12], in such an FBL regime, the communication is no longer error-free even if setting the coding rate is lower than the Shannon capacity, and the FBL impacts should be considered in the latency-critical system design.

Nevertheless, several studies have taken the FBL impacts into account while improving the network's EE performance. The work in [13] considers a multi-node scenario that introduces an unsupervised learning-based power allocation on maximizing EE for transmissions in the FBL regime. In addition, reference [14] maximizes EE by jointly determining subcarrier and transmit power. All the above existing works address the EE enhancement from only the perspective of determining the transmit power. Note that the energy consumption of transmitting a packet is influenced by both transmit power and transmission blockength. To the best of our knowledge, the impacts of the joint blocklength and power allocation among multi-nodes on the overall system EE has not been well-studied, while an EE maximization design via such joint resource allocation in the FBL regime is still an open question.

In this work, we consider an industrial IoT network sup-

Y. Hu is the corresponding author. This work was supported in part by the National Key R&D Program of China under Grant 2023YFE0206600, and in part by the Fundamental Research Funds for the Central Universities (2042024kf1006), and in part by the Federal Ministry of Education and Research of Germany in the project "Open6GHub" (grant number: 16KISK012).

porting transmissions in the FBL regime and propose an EE maximization design. Our contributions are

- We provide an EE maximizing design via efficiently jointly allocating the power and blocklength among the transmissions to different nodes, while guaranteeing per-node constraint of reliability. A Majorization-Minimization-based algorithm is introduced achieving a near-optimal solution.
- For each local point during the algorithm, a tightly approximated local problem is conducted. We rigorously prove the joint convexity of the transmission error rate with respect to the power and blocklength, following which each local problem can be optimally solved.

The rest of the paper is structured as follows. In Section II, we describe the system model and the communication performance model in the FBL regime. In Section III, We formulate the joint optimization problem for EE and derive the approximate convex problem of each local problem. Section IV provides the simulation results and conclusions are offered in Section V.

II. Preliminaries

In this section, we first present the system model, followed by a review of the FBL communication performance model.

A. System Model

We consider a multi-node IoT system with an access point and J user nodes as shown in Fig. 1. The system operates in a time-slotted manner under time division multiple access (TDMA). The time is divided into frames with length of $M_{\max}T_{\mathrm{s}}$, where T_{s} is the time length of each symbol and $M_{\max}$ is the number of symbols in each frame. The value of $M_{\max}$ can not be set too large due to the low latency requirements of the served multiple nodes. Denote by m_j the blocklength (number of symbols) allocated to node j in a frame, then we have $\sum_{j=1}^{J} m_j \leq M_{\max}$.

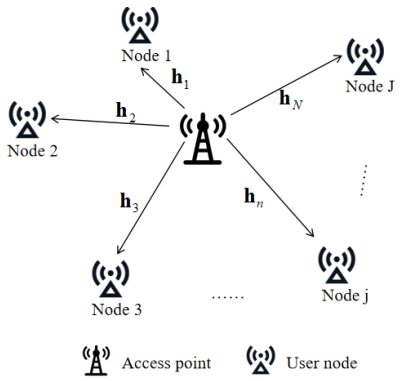

Fig. 1. An example of the considered IoT networks.

Assume the channels to experience quasi-static fading. Denote the channel gain from the AP to node j by h_j. Then, the corresponding received signal-to-noise ratio (SNR) at node j can be written as

$$\gamma_j = \frac{p_j h_j}{\sigma^2}, \tag{1}$$

where p_j denotes the transmit power and h_j denotes the channel gain. σ^2 is the noise spectral density. In this paper, we assume the channel obeys a Rayleigh distribution.

The packet size of node j is k_j. Hence, the total amount data is $\sum_{j=1}^{J} k_j$, and the total energy consumption is $T_{\mathrm{s}} \sum_{j=1}^{J} m_j p_j$. Then, the EE can be formulated as the average amount of data that can be transmitted per unit of energy:

$$\eta = \frac{\sum_{j=1}^{J} k_j}{T_s \sum_{j=1}^{J} m_j p_j}. \tag{2}$$

B. FBL Communication Performance Model

As the transmission is carried out in the FBL regime, the transmission error rate is comparable, even if the coding rate is below Shannon's capacity. To ensure the quality of communication service, each node has a corresponding upper requirement $\epsilon_{j,\max}$ for its error rate ϵ_j.

On the basis of [12], the decoding error probability under FBL codes with a coding rate $r_j = \frac{k_j}{m_j}$ is given by

$$\epsilon_j \approx \mathcal{Q}\left(\sqrt{\frac{m_j}{\mathcal{V}(\gamma_j)}}\left(\mathcal{C}\left(\gamma_j\right) - r_j\right)\right), \tag{3}$$

where Shannon's capacity $\mathcal{C}\left(\gamma_j\right) = \log_2(1+\gamma_j)$, and the channel dispersion $\mathcal{V}(\gamma_j) = \left(1-\left(1+\gamma_j\right)^{-2}\right)\left(\log_2 e\right)^2$. Gaussian Q-function $\mathcal{Q}(x) = \int_x^{\infty} \frac{1}{\sqrt{2\pi}} e^{-\frac{y^2}{2}} dy$.

III. Energy Efficiency Maximization Design

In this section, we propose a novel EE maximization design via jointly allocating transmit power and blocklength among nodes. Specifically, we start with the problem formulation. Subsequently, a Majorization-Minimization-based approach is proposed for the constructed non-convex problem. We tightly approximate the problem at each local point and a rigorous proof of the convexity of the local problem is provided. Finally, the whole algorithm is presented.

A. Problem Formulation

The original problem (OP) maximizing the EE via jointly determining the power and blocklength is formulated as follows:

$$(\mathrm{OP}): \max_{\mathbf{m},\mathbf{p}} \quad \frac{\sum_{j=1}^{J} k_j}{T_{\mathrm{s}} \sum_{j=1}^{J} m_j p_j} \tag{4a}$$

$$\text{s.t.}: \sum_{j=1}^{J} m_j \leq M_{\max}, \tag{4b}$$

$$m_j \in \mathbb{N}^+, \forall j = 1, \cdots, J, \tag{4c}$$

$$0 < p_j \leq p_{\max}, \forall j = 1, \cdots, J, \tag{4d}$$

$$\epsilon_j \leq \epsilon_{j,\max}, \forall j = 1, \cdots, J. \tag{4e}$$

where $\mathbf{m} = \{m_1, \cdots, m_J\}$ and $\mathbf{p} = \{p_1, \cdots, p_J\}$ are the blocklength allocation and power allocation decision vectors, respectively. $p_{\max}$ is the maximum power that one node is allowed to be allocated. Constraint (4e) ensures the per-node reliability requirement.

Problem (OP) is non-convex as a result of the non-convexity characteristics of the objective function (4a) and of constraint (4e), which makes directly solving the problem challenging.

B. Efficient Solution to (OP)

With given k_j and T_s as constants, Problem (OP) is actually equivalent to minimizing $\sum_{j=1}^{J} m_j p_j$. However, this new objective function is still non-convex. To solve this difficulty, we conduct a function $F^\tau(\mathbf{p},\mathbf{m})$ as

$$F^\tau(\mathbf{p},\mathbf{m}) = \frac{C^\tau}{2} + \frac{1}{2C^\tau}\left(\sum_{j=1}^{J} m_j p_j\right)^2, \tag{5}$$

where $C^\tau > 0$ is an auxiliary constant.

In the light of the Cauchy-Buniakowsky-Schwarz inequality, we have

$$\sum_{j=1}^{J} m_j p_j \le F^\tau(\mathbf{p},\mathbf{m}), \tag{6}$$

where the equality holds only if $C^\tau = \sum_{j=1}^{J} m_j p_j$.

For each node, relaxing the integer variables m_j, $\forall j = 1,\cdots,J$ into continuous variables, constraint (4e) can be rewritten as:

$$f(x,y) \triangleq -\frac{\log_2 x - ky^{-1}}{\sqrt{y^{-1}(1-x^{-2})}} \le -\mathcal{Q}^{-1}(\epsilon_{j,\max})\log_2 e, \tag{7}$$

where $x = 1+\gamma_j > 1$ and $y = m_j > 0$.

Therefore, the problem at local point $(\mathbf{p}^\tau,\mathbf{m}^\tau)$ can be tightly approximated to the following approximated local problem (LP) with $C^\tau = \sum_{j=1}^{J} m_j^\tau p_j^\tau$:

$$\begin{aligned}
(\mathrm{LP}):\ \min_{\mathbf{m},\mathbf{p}}\quad & F^\tau(\mathbf{p},\mathbf{m}) && \text{(8a)}\\
\text{s.t.}:\ & \sum_{j=1}^{J} m_j \le M_{\max}, && \text{(8b)}\\
& 0 < p_j \le p_{\max}, \forall j = 1,\cdots,J, && \text{(8c)}\\
& f(1+\gamma_j, m_j) \le -\mathcal{Q}^{-1}(\epsilon_{j,\max})\log_2 e, \\
& \forall j = 1,\cdots,J. && \text{(8d)}
\end{aligned}$$

After that, we have the key lemma shown following to address Problem (LP).

Lemma 1. *Problem (LP) is convex, when $\gamma_j \ge \gamma_0$, $\forall j = 1,\cdots,J$.*

Proof. The Hessian matrix of the conducted objective function $F^\tau(\mathbf{p},\mathbf{m})$ is

$$\mathbf{H}_{F^\tau} = \frac{1}{C^\tau}\begin{bmatrix}
m_1^2 & m_1m_2 & \cdots & m_1p_1 & \cdots & m_1p_J\\
m_2m_1 & m_2^2 & \cdots & m_2p_1 & \cdots & m_2p_J\\
\vdots & \vdots & \ddots & \vdots & \ddots & \vdots\\
p_1m_1 & p_1m_2 & \cdots & p_1^2 & \cdots & p_1p_J\\
\vdots & \vdots & \ddots & \vdots & \ddots & \vdots\\
p_Jm_1 & p_Jm_2 & \cdots & p_Jp_1 & \cdots & p_J^2
\end{bmatrix}, \tag{9}$$

which is a Gram matrix, so it is a positive semi-definite matrix according to the Gram matrix's properties. Therefore, $F^\tau(\mathbf{p},\mathbf{m})$ is convex.

Note that constraints (8b) and (8c) are linear. Hence, the remaining task is to show the convexity of (8d). In the following, we prove this by showing that the Hessian matrix of the function $f(x,y)$ given in (7) is a positive semi-definite. The Hessian matrix is given below:

$$\mathbf{H}_f = \begin{bmatrix}
\dfrac{\partial^2 f}{\partial x^2} & \dfrac{\partial^2 f}{\partial x\partial y}\\
\dfrac{\partial^2 f}{\partial x\partial y} & \dfrac{\partial^2 f}{\partial y^2}
\end{bmatrix}. \tag{10}$$

First of all, the first order leading principal minor of $\mathbf{H}_f$ is

$$\begin{aligned}
\frac{\partial^2 f}{\partial x^2} =& (x^2-1)^{-5/2}xy^{1/2}\left[3ky^{-1} - \right.\\
& \left. 3\log_2 x + (x^2 - x^{-2})\log_2 e\right].
\end{aligned} \tag{11}$$

Let

$$g_1(x) = -3\log_2 x + (x^2 - x^{-2})\log_2 e. \tag{12}$$

As $(x^2-1)^{-5/2}xy^{1/2} > 0$ and $3ky^{-1} > 0$ hold, in the following we show $\frac{\partial^2 f}{\partial x^2} > 0$ by proving $g_1(x) \ge 0$.

According to $\ln x \le x-1$, $\forall x > 0$, it is easy to derive that $\log_2 x \le (x-1)\log_2 e$, $\forall x > 0$. Then, we have

$$g_1(x) \ge x^{-2}(x^4 - 3x^3 + 3x^2 - 1)\log_2 e. \tag{13}$$

Let

$$q_1(x) = x^4 - 3x^3 + 3x^2 - 1. \tag{14}$$

To determine the range of $g_1(x)$, we need to analyze $q_1(x)$ first. The first derivative of $q_1(x)$ is

$$q_1'(x) = 4x^3 - 9x^2 + 6x, \tag{15}$$

and the second derivative is

$$q_1''(x) = 6(x-1)(2x-1). \tag{16}$$

Noted that $q_1''(x) > 0$ and $q_1'(x) > 0$ for $x > 1$, we have $q_1(x) > 0$. As a result, $g_1(x) > 0$ holds.

So far, we conclude that the first order leading principal minor of the matrix $\mathbf{H}_f$ is positive.

Next, the second order leading principal minor of $\mathbf{H}_f$ is

$$\begin{aligned}
&\frac{\partial^2 f}{\partial x^2}\frac{\partial^2 f}{\partial y^2} - \left(\frac{\partial^2 f}{\partial x\partial y}\right)^2\\
=&\frac{1}{4}y^{-1}(x^2-1)^{-3}\left\{x^2(\log_2 x + 3ky^{-1})[3ky^{-1} - 3\log_2 x + \right.\\
&\left.(x^2 - x^{-2})\log_2 e] - (\log_2 x + ky^{-1} - x^2\log_2 e + \log_2 e)^2\right\}.
\end{aligned} \tag{17}$$

By introducing auxiliary variable $z = ky^{-1} > 0$, (17) can be rewritten as

$$\frac{\partial^2 f}{\partial x^2}\frac{\partial^2 f}{\partial y^2} - \left(\frac{\partial^2 f}{\partial x\partial y}\right)^2 = \frac{1}{4}y^{-1}(x^2-1)^{-3}g_2(x,z), \tag{18}$$

Algorithm 1 : Algorithm to solve (OP).

Initialization

Initialize a feasible point $(\mathbf{p}^0, \mathbf{m}^0)$, the number of nodes J, and set $\tau = 0$.

Iteration

a) Calculate $F^\tau(\mathbf{p}, \mathbf{m})$ and build up convex problem (LP);

b) Solve the convex problem (LP) and obtain local optimal solution $(\mathbf{p}^\star, \mathbf{m}^\star)$;

c) If performance improvement $<$ threshold
stop iteration and return $(\mathbf{p}^\star, \mathbf{m}^\star)$;
Else
$(\mathbf{p}^{\tau+1}, \mathbf{m}^{\tau+1}) = (\mathbf{p}^\star, \mathbf{m}^\star)$; $\tau = \tau + 1$;
return to **a).**

where

$$g_2(x,z) = x^2(\log_2 x + 3z)[3z - 3\log_2 x + (x^2 - x^{-2})\log_2 e] - (\log_2 x + z - x^2 \log_2 e + \log_2 e)^2. \quad (19)$$

Proposition 1. $g_2(x,z) > 0$

Proof. the proof is given in the appendix □

With the proposition, (18) is positive as $\frac{1}{4}y^{-1}(x^2-1)^{-3} > 0$. Further, the second order leading principal minor of the matrix $\mathbf{H}_f$ is positive:

$$\frac{\partial^2 f}{\partial x^2}\frac{\partial^2 f}{\partial y^2} - \left(\frac{\partial^2 f}{\partial x \partial y}\right)^2 > 0, x > x_0. \quad (20)$$

On account of the definition that $x = 1 + \gamma_j$, there is $x_0 = 1 + \gamma_0$ with $\gamma_0 = 1.5$.

Hence, the convexity of the Problem (LP) is assured due to the fact that the error probability ϵ_n is jointly convex in $\mathbf{p}$ and $\mathbf{m}$, alongside the objective function in Problem (LP) is jointly convex as well. □

Following the lemma, Problem (LP) is convex when $\gamma_j > \gamma_0$ which is under practical interests of reliable communications in the considered industrial IoT network. The optimal solution of (LP) can be efficiently solved by using standard convex programming methods, such as the ellipsoid method [15]. To ensure the transmission reliability, the m_j, $\forall j = 1, \cdots, J$ obtained by convex optimization needs to be rounded up as $\lceil m_j \rceil$.The entire process of jointly optimizing the transmit power and blocklength is presented in Algorithm 1.

IV. Simulation Results

In this section, through Monte Carlo simulations we evaluate the EE performance of the proposed design in comparison to benchmarks, i.e., performing pure power allocation (transmissions with the same blocklength) or pure blocklength allocation (with equal transmit power). In the simulation, we set the channel to satisfy Rayleigh fading with the location of the nodes generated randomly, and the noise spectral density to $\sigma^2 = 10^{-7}$. Besides, we set the maximal transmit power to $p_{\max} = 10$ W, and the reliability requirements to $\epsilon_{j,\max} = \epsilon_{\max} = 10^{-3}$, $\forall j = 1, ..., J$. Meanwhile, set the packet transmitted to each node to the same size k. The setting for k and $M_{\max}$ is discussed in the following simulations.

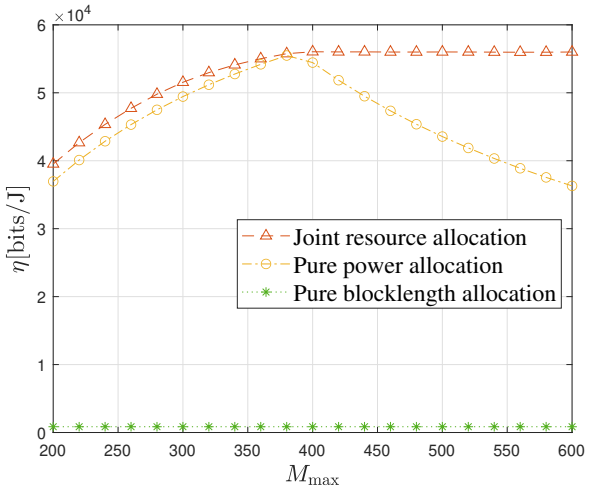

Fig. 2. EE against the number of symbols per frame $M_{\max}$. In the simulation, we set $J = 2$ nodes and packet size $k = 200$ bits.

We start with Fig. 2 to investigate the advantage of the joint design on the varies of the frame length. It can be observed that our proposed algorithm outperforms the benchmarks, which shows the benefit of the joint design. As shown in the picture, the EE performance of the pure blocklength design scheme exhibits poor performance, showing no improvement with the increase in the total blocklength M_{max}. This observation can be elucidated through constraint (4e), i.e., the minimum blocklength $m_{j,\min}$ required for node j satisfies the equation below:

$$\mathcal{C}(\gamma_j)m_{j,\min} - \mathcal{V}(\gamma_j)\mathcal{Q}^{-1}(\epsilon_{\max})(\log_2 e)m_{j,\min}^{1/2} - k_j = 0, \quad (21)$$

which is independent of $M_{\max}$ with equal power. Furthermore, compared with the pure power design scheme curve, the proposed algorithm consistently demonstrates superior performance. Notably, the performance gap widens as $M_{\max}$ increases. Specifically, within a low region of $M_{\max}$, the proposed algorithm shows certain advantages over the pure power design, as the part of blocklength allocation lacks sufficient leeway to perform a significant role. Conversely, within a high region of $M_{\max}$, the proposed design shows notable superiority over the pure power design, attributable to ample scope for joint optimization. Moreover, we can observe that although the pure power design is capable of reaching good performance, its curve of EE first increases and then decreases. By contrast, the proposed design experiences an initial increase followed by maintenance at a stable level. This is because the pure power design divides the blocklength equally, while the proposed design can choose a better allocation according to the change of $M_{\max}$. This further reveals the adaptability of the joint design to total blocklength resources.

Next, we analyze the impact of the packet size k on the EE. As shown in Fig. 3, the proposed algorithm outperforms the benchmarks. In particular, except for the pure blocklength design scheme, both the proposed design's and the pure power design's curves increase first and then decrease. Because more

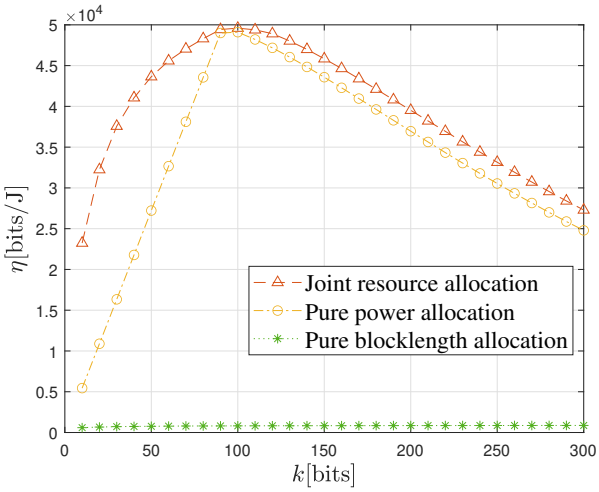

Fig. 3. EE against the packet size k received by each node. In the simulation, we set $J = 2$ nodes and the number of symbols per frame $M_{\max} = 200$.

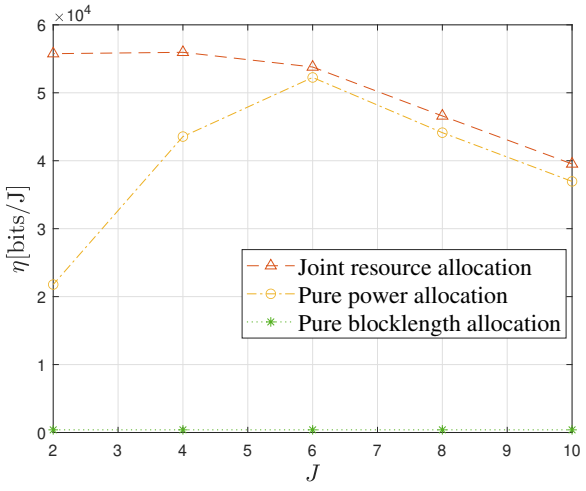

Fig. 4. EE against the number of nodes J. In the simulation, we set packet size $k = 200$ bits and the number of symbols per frame $M_{\max} = 1000$.

k means more bits transmitted per energy, while too much k means more energy is needed to guarantee transmission reliability. As for the pure blocklength design, we can see that the curve has a very small lift when k is small, and then it is almost unchanged. This can be interpreted by solving (21) and get

$$\frac{m_{j,\min}}{k} = (2\mathcal{C}(\gamma_j))^{-2}\left[\mathcal{V}(\gamma_j)^{-1/2}\mathcal{Q}^{-1}(\epsilon_{\max})(\log_2 e)k^{-1/2} + \sqrt{\mathcal{V}(\gamma_j)k_j^{-1} + 4\mathcal{C}(\gamma_j)}\right]^2, \tag{22}$$

i.e., when k reaches a certain value, the EE is mainly determined by the constant term in (22). In addition, we can observe that the proposed design shows a significantly higher performance than the pure power design in a low region of k. In a high region of k, however, the proposed design only shows a certain advantage over the pure power design on EE. This is because the smaller the packet size is, the shorter blocklength is needed for reliability, i.e., the lower the minimal blocklength allowed is, leading to ample scope for blocklength's choice in joint allocation. Furthermore, even though the highest values of EE of the proposed design and the pure power design are relatively close, it can be seen that the curve of the proposed design crosses the highest point smoothly, while that of the pure power design is more sensitive around the highest point. This indicates that our proposed design is more robust and less sensitive to the choices of packet size k.

Finally, the advantage of the proposed design with variations in the number of nodes J is depicted in Fig. 4. Clearly, the proposed design performs better than the two benchmarks. Besides, it is observed that the EE curves perform differently as J increases. The curve of pure blocklength design is still at a poor level (such a feature is also present in Fig. 2 and Fig. 3), since it has no optimization for power, while the power needed can vary across orders of magnitude as the channel changes. The curve of pure power design first rises due to an increase in the amount of transmitted data and then falls resulting from resource consumption increasing significantly with more nodes. While the curve of our proposed design presents a monotonically decreasing process. And it decreases very slowly with a small number of nodes. This demonstrates that the proposed design can achieve a higher performance especially when J is small. When J is large, our proposed design is still better than the pure power design, although it is also decreasing.

V. Conclusion

In this paper, we investigated EE for multi-node IoT networks in the FBL regime. We proposed a joint power and blocklength allocation design targeting maximizing the EE. However, the constructed joint optimization problem is non-convex, so we adopted a Majorization-Minimization-based approach. Each local problem was investigated and tightly approximated to a convex one. Finally, a near-optimal solution was achieved. Via simulation, we validated the benefit and robustness of the joint resource allocation design. The proposed approach can be extended to scenarios with more requirements, such as the minimum coding rate requirement.

References

[1] R. Chen, M. Liu, Y. Hui, N. Cheng, and J. Li, "Reconfigurable intelligent surfaces for 6G IoT wireless positioning: A contemporary survey," *IEEE Internet Things J.*, vol. 9, no. 23, pp. 23 570–23 582, 2022.

[2] D. C. Nguyen, M. Ding, P. N. Pathirana, A. Seneviratne, J. Li, D. Niyato, O. Dobre, and H. V. Poor, "6G internet of things: A comprehensive survey," *IEEE Internet Things J.*, vol. 9, no. 1, pp. 359–383, 2022.

[3] Y. Huang, L. Liu, J. Yu, Y. Fang, and W. Gong, "Energy-efficient wifi backscatter communication for green IoTs," in *GLOBECOM 2023 - 2023 IEEE Global Communications Conference*, 2023, pp. 6207–6212.

[4] J. Premalatha and A. S. Anselin Nisha, "Energy efficient transmission in cellular network using time reversal for green communication," in *2021 International Conference on Advances in Electrical, Computing, Communication and Sustainable Technologies (ICAECT)*, 2021, pp. 1–5.

[5] F. Yassine, M. El Helou, S. Lahoud, and O. Bazzi, "Performance of narrowband IoT link adaptation with rate and energy objectives," in *2021 IEEE 3rd International Multidisciplinary Conference on Engineering Technology (IMCET)*, 2021, pp. 6–10.

[6] Y. He, S. Zhang, L. Tang, and Y. Ren, "Large scale resource allocation for the internet of things network based on ADMM," *IEEE Access*, vol. 8, pp. 57 192–57 203, 2020.
[7] X. Zhang, H. Qi, X. Zhang, and L. Han, "Energy-efficient resource allocation and data transmission of cell-free internet of things," *IEEE Internet Things J.*, vol. 8, no. 20, pp. 15 107–15 116, 2021.
[8] K. Wang, P. Wu, and M. Xia, "Energy-efficient scheduling and resource allocation for power-limited cognitive IoT devices," in *2023 19th International Conference on Wireless and Mobile Computing, Networking and Communications (WiMob)*, 2023, pp. 104–109.
[9] O. Yang and Y. Wang, "Optimization of time and power resources allocation in communication systems under the industrial internet of things," *IEEE Access*, vol. 8, pp. 140 392–140 398, 2020.
[10] G. Ozcan and M. C. Gursoy, "Throughput of cognitive radio systems with finite blocklength codes," *IEEE J. Sel. Areas Commun.*, vol. 31, no. 11, pp. 2541–2554, 2013.
[11] X. Chen, D. W. K. Ng, W. Yu, E. G. Larsson, N. Al-Dhahir, and R. Schober, "Massive access for 5G and beyond," *IEEE J. Sel. Areas Commun.*, vol. 39, no. 3, pp. 615–637, 2021.
[12] Y. Polyanskiy, H. V. Poor, and S. Verdu, "Channel coding rate in the finite blocklength regime," *IEEE Trans. Inf. Theory.*, vol. 56, no. 5, pp. 2307–2359, 2010.
[13] H. Zhao, B. Xu, Q. Wang, H. Huang, and X. Zhang, "Unsupervised learning for energy efficient power allocation in ultra-reliable and low-latency communications," in *2022 IEEE 96th Vehicular Technology Conference (VTC2022-Fall)*, 2022, pp. 1–5.
[14] K. Singh, M.-L. Ku, and M. F. Flanagan, "Energy-efficient precoder design for downlink multi-user miso networks with finite blocklength codes," *IEEE Trans. Green Commun. Netw*, vol. 5, no. 1, pp. 160–173, 2021.
[15] P. Stetsyuk, A. Fischer, and O. Khomyak, "The generalized ellipsoid method and its implementation," in *Optimization and Applications*, M. Jaćimović, M. Khachay, V. Malkova, and M. Posypkin, Eds. Cham: Springer International Publishing, 2020, pp. 355–370.
[16] D. Kathy, P. Helmut, and S. Carsten, "Padé approximations to the logarithm II: Identities, recurrences, and symbolic computation," Ramanujan J 11, 139–158 (2006), https://doi.org/10.1007/s11139-006-6503-4.

APPENDIX

The first partial derivative of $g_2(x,z)$ with respect to z is calculated as

$$\begin{aligned}\frac{\partial g_2}{\partial z} =&3x^2(3z-3\log_2 x+x^2\log_2 e-x^{-2}\log_2 e)+\\ &3x^2(\log_2 x+3z)-2(\log_2 x+z-x^2\log_2 e+\log_2 e).\end{aligned} \tag{23}$$

The second partial derivative of $g_2(x,z)$ with respect to z is calculated as

$$\frac{\partial^2 g_2}{\partial z^2}=18x^2-2. \tag{24}$$

Clearly, $\frac{\partial^2 g_2}{\partial z^2}>0$ when $x>1$, i.e., $\frac{\partial g_2}{\partial z}>\frac{\partial g_2}{\partial z}|_{z=0}$ holds with $z>0$. $\frac{\partial g_2}{\partial z}|_{z=0}$ is calculated as

$$\begin{aligned}\left.\frac{\partial g_2}{\partial z}\right|_{z=0} =&(3x^4-6x^2\ln x+2x^2-2\ln x-5)\log_2 e\\ =&q_2(x)\log_2 e,\end{aligned} \tag{25}$$

with $q_2(x)=3x^4-6x^2\ln x+2x^2-2\ln x-5$. The first derivative of the function $q_2(x)$ is calculated as

$$\begin{aligned}q_2'(x)=&12x^3-12x\ln x-2x-2x^{-1}\\ \overset{\ln x\le x-1}{\geq}&12x^2(x-1)+2x^{-1}(5x^2-1)\\ \overset{x\ge 1}{>}&0,\end{aligned} \tag{26}$$

so $q_2(x)>0$ holds with $x>1$. Recalling (25), $\frac{\partial g_2}{\partial z}|_{z=0}>0$. Consequently, $\frac{\partial g_2}{\partial z}>0$. Thus,

$$\begin{aligned}g_2(x,z)>&g_2(x,0)\\ =&\left[x^4\ln x-3x^2(\ln x)^2-\ln x-\right.\\ &\left.(\ln x-x^2+1)^2\right](\log_2 e)^2\end{aligned} \tag{27}$$

holds. Let

$$q_3(x)=x^4\ln x-3x^2(\ln x)^2-\ln x-(\ln x-x^2+1)^2. \tag{28}$$

Therefore, $g_2(x,z)>0$ holds if $q_3(x)>0$.

The first derivative of $q_3(x)$ is calculated and sorted as

$$\begin{aligned}q_3'(x)=&4x^3\ln x-3x^3-6x(\ln x)^2-2x\ln x+6x-\\ &2x^{-1}\ln x-2x^{-1}.\end{aligned} \tag{29}$$

Note that $\ln x\le x-1$ holds. Then, we have $6x(\ln x)^2<6x(2\sqrt{x}-2)\ln x$. Accordingly,

$$\begin{aligned}q_3'(x)>&(4x^3-12x^{3/2}+10x-2x^{-1})\ln x-\\ &3x^3+6x-2x^{-1}.\end{aligned} \tag{30}$$

In order to prove that the right-hand side of the inequality (30) is positive, it is necessary to determine that the coefficients of $\ln x$ are positive. Let

$$q_4(x)=4x^3-12x^{3/2}+10x-2x^{-1}. \tag{31}$$

Calculate the first and the second derivatives of $q_4(x)$ as follows

$$\begin{aligned}q_4'(x)=&12x^2-18x^{1/2}+2x^{-2}+10,\\ q_4''(x)=&24x-9x^{-1/2}-4x^{-3}.\end{aligned} \tag{32}$$

Obviously, $q_4''(x)>0$ with $x>1$. Similarly, $q_4'(x)>0$ and $q_4(x)>0$, so the coefficients of $\ln x$ is positive.

According to Pade approximation [16] of logarithm, there is $\ln x\ge\frac{2(x-1)}{x+1}$. Applying it to (30), we get

$$\begin{aligned}q_3'(x)>&(x+1)^{-1}(5x^4-11x^3-24x^{5/2}+\\ &26x^2+24x^{3/2}-14x+2x^{-1}-6).\end{aligned} \tag{33}$$

Let

$$\begin{aligned}q_5(x)=&5x^4-11x^3-24x^{5/2}+\\ &26x^2+24x^{3/2}-14x+2x^{-1}-6.\end{aligned} \tag{34}$$

The first, second and third derivatives of $q_5(x)$ are calculated as follows:

$$q_5'(x)=20x^3-33x^2-60x^{3/2}+52x+36x^{1/2}-14-2x^{-2}, \tag{35}$$

$$q_5''(x)=60x^2-66x-90x^{1/2}+52+18x^{-1/2}+4x^{-3}, \tag{36}$$

$$q_5'''(x)=120x-66-45x^{-1/2}-9x^{-3/2}-12x^{-4}. \tag{37}$$

Take the range that $x\ge x_0$ and let $x_0=2.5$. Then it exists that $q_5'''(x)\ge q'''(x_0)>0$. Similarly, $q_5''(x)>0$, $q_5'(x)>0$ as well as $q_5(x)>0$.

Equivalently, we have $q_3'(x)>0$ according to (33) and (34). Therefore, $q_3(x)>q_3(x_0)=0.35>0$. Based on (27) we can obtain that $g_2(x,z)>0$ holds with $x\ge x_0$.